

Neutrino oscillation in Magnetized Gamma-Ray Burst Fireball

Sarira Sahu¹, Nissim Fraija¹ and Yong-Yeon Keum^{2,3}

¹*Instituto de Ciencias Nucleares, Universidad Nacional Autónoma de México, Circuito Exterior, C. U., A. Postal 70-543, 04510 México DF, México*

²*Asia Pacific Center for Theoretical Physics POSTECH, San-31, Hyoja-Dong, NamKu, Pohang, Gyeongbuk 790-784 Korea,*

³*Department of Physics and BK21 Initiative for Global Leaders in Physics, Korea University, Seoul 136-701, Korea*

Neutrinos of energy about 5-20 MeV are produced due to the stellar collapse or merger events that trigger the Gamma-Ray Burst. Also low energy MeV neutrinos are produced within the fireball due to electron positron annihilation and nucleonic bremsstrahlung. Many of these neutrinos will propagate through the dense and relativistic magnetized plasma of the fireball. We have studied the possibility of resonant oscillation of $\nu_e \leftrightarrow \nu_{\mu,\tau}$ by taking into account the neutrino oscillation parameters from SNO, SuperKamiokande and Liquid Scintillator Detector. Using the resonance condition we have calculated the resonance length for these neutrinos and also the fireball observables like lepton asymmetry and the baryon load are estimated based on the assumed fireball radius of 100 Km.

I. INTRODUCTION

Gamma-Ray Bursts (GRBs) are flashes of non-thermal bursts of low energy (~ 100 KeV-1 MeV) photons and release about 10^{51} - 10^{53} erg in a few seconds making them the most luminous object in the universe after the Big Bang[1, 2]. They have cosmological origin[1, 2, 3, 4] and fall into two classes: short-hard bursts (≤ 2 s) and long-soft bursts. It is now widely accepted that long duration bursts are produced due to the core collapse of massive stars the so called hypernovae [1, 5, 6]. The origin of short-duration bursts are still a mystery, but recently there has been tremendous progress due to accurate localization of many short bursts by the Swift[7, 8] and HETE-2[9] satellites and the observations seem to support the coalescing of compact binaries as the progenitor for the short-hard bursts. Recently millisecond magnetars have been considered as possible candidates as the progenitor for the short-hard bursts[10, 11].

Irrespective of the nature of the progenitor, it is believed that, gamma-ray emission arises from the collision of different internal shocks (shells) due to relativistic outflow from the source. A class of models called *fireball model* seems to explain the temporal structure of the bursts and the non-thermal nature of their spectra[1, 2, 3, 12, 13]. A major setback of this approach is its inability to explain the late activity of the central engine[14, 15].

In the standard fireball scenario, a radiation dominated plasma is formed in a compact region with a size $c\delta t \sim 100$ -1000 km[1, 13]. This creates an opaque $\gamma - e^\pm$ fireball due to the process $\gamma + \gamma \rightarrow e^+ + e^-$. The average optical depth of this process is $\tau_{\gamma\gamma} \simeq 10^{13}$. Because of this huge optical depth, photons can not escape freely and even if there are no pairs to begin with, they will form very rapidly and will Compton scatter lower energy photons. In the fireball the γ and e^\pm pairs will thermalize with a temperature of about 3-10 MeV. The fireball expands relativistically with a large Lorentz factor and cools adiabatically due to the expansion. The radiation emerges freely to the inter stellar medium (ISM), when the optical depth is $\tau_{\gamma\gamma} \simeq 1$. In addition to γ , e^\pm pairs, fireball may also contain some baryons, both from the progenitor and the surrounding medium and the electrons associated with the matter (baryons) can increase the opacity, hence delaying the process of emission of radiation.

As discussed above, core collapse of massive stars, merger of binary compact objects (neutron star-neutron star, neutron star-black hole) and millisecond magnetars as possible progenitors of the long and short GRBs respectively. The process of collapse in all these scenarios are similar to the one that takes place in supernovae of type II and neutrinos of energy 5-20 MeV are produced. Also due to nucleonic bremsstrahlung $NN \rightarrow NN\nu\bar{\nu}$ as well as electron positron annihilation $e^+e^- \rightarrow Z \rightarrow \nu\bar{\nu}$, neutrinos of all the three flavors can be produced during the merger process[16]. Fractions of these neutrinos will be able to propagate through the fireball formed far away from the central engine. Within the fireball the inverse beta decay of proton $p + e^- \rightarrow n + \nu_e$ will also produce MeV neutrinos which then propagate through it. From the accretion disc neutrinos of similar energy are radiated as discussed in the ref.[6] and fractions of these neutrinos may also pass through the fireball if the accreting materials survive for longer period. In the fireball picture, a substantial fraction of the baryon kinetic energy is transferred to a non-thermal population of electrons through Fermi acceleration at the shock and these accelerated electrons will cool through synchrotron emission and/or inverse Compton scattering to produce observed emission in prompt and afterglow phase. The synchrotron emission from relativistic electrons take place either in a globally ordered magnetic field which was probably carried from the central engine or in random magnetic fields generated in the shock dissipation region. But it is difficult to estimate the strength of the magnetic field from the first principle. However polarization information

of the GRBs, if retrieved, would give valuable information regarding the magnetic field and the nature of the central engine.

The neutrino properties get modified when it propagates in a medium. Even a massless neutrino acquires an effective mass and an effective potential in the medium. The resonant conversion of neutrino from one flavor to another due to the medium effect is important for solar neutrinos which is well known as the MSW effect. Similarly the propagation of neutrino in the early universe hot plasma[17], supernova medium[18] and in the GRB fireball[19] can have also many important implications in their respective physics. The magnetic field is intrinsically entangled with the matter in all the above scenarios. Although neutrino can not couple directly to the magnetic field, its effect can be felt through coupling to charge particles in the background. Neutrino propagation in a neutron star in the presence of a magnetic field and also in the magnetized plasma of the early universe has been studied extensively. But to the best of our knowledge, there exist no work on the propagation of neutrino in a magnetized fireball plasma and we believe that the combine effect of matter and magnetic field will give interesting effect. In this context, we have studied the propagation of low energy MeV neutrinos in the magnetized plasma of the GRB fireball.

The paper is organized as follows: We derive the effective potential for a neutrino in the presence of a weakly magnetized electron positron plasma in sec. 2. In sec. 3, the effective potential for extremely strong field limit is discussed. We discuss about the physics of GRB in sec. 4 and sec. 5 is devoted to the oscillation of neutrinos in GRB environment by taking into account the results from SNO, SuperKamiokande and LSND. A brief conclusion is given in sec. 6.

II. NEUTRINO POTENTIAL

The neutrino propagation in a heat bath has been studied extensively[17, 20]. Using the finite temperature field theory method and considering the effect of magnetic field through Schwinger's propertime method, the effective potential of a propagating neutrino is derived in a magnetized medium[21], which can be given by,

$$V_{\text{eff}} = b - c \cos \phi + (a_{\parallel} - a_{\perp})|\mathbf{k}| \sin^2 \phi \quad (2.1)$$

where a , b and c are the Lorentz scalars. For an electron neutrino propagating in the above medium, the scalar functions are given by

$$a_{\parallel} = -\frac{g^2 e B}{M_W^4} \int_0^{\infty} \frac{dp_3}{(2\pi)^2} \sum_{n=0}^{\infty} (2 - \delta_{n,0}) \frac{m^2}{E_{e,n}} (f_{e,n} + \bar{f}_{e,n}) + \frac{g^2}{4M_W^4} \left(k_3(N_e^0 - \bar{N}_e^0) + k_0(N_e - \bar{N}_e) \right), \quad (2.2)$$

$$a_{\perp} = -\frac{g^2 e B}{M_W^4} \int_0^{\infty} \frac{dp_3}{(2\pi)^2} \sum_{n=0}^{\infty} (2 - \delta_{n,0}) \left(\frac{2neB}{2E_{e,n}} + \frac{m^2}{E_{e,n}} \right) (f_{e,n} + \bar{f}_{e,n}) + \frac{g^2}{4M_W^4} \left(k_3(N_e^0 - \bar{N}_e^0) + k_0(N_e - \bar{N}_e) \right), \quad (2.3)$$

$$b = \frac{g^2}{4M_W^2} (N_e - \bar{N}_e)(1 + c_V) + \frac{g^2 e B}{4M_W^4} (N_e^0 - \bar{N}_e^0) - \frac{e B g^2}{M_W^4} \int_0^{\infty} \frac{dp_3}{(2\pi)^2} \sum_{n=0}^{\infty} (2 - \delta_{n,0}) \left[\frac{k_3}{E_{e,n}} (p_3^2 + \frac{m^2}{2}) \delta_{n,0} + E_{\nu_e} E_{e,n} \right] (f_{e,n} + \bar{f}_{e,n}), \quad (2.4)$$

$$c = \frac{g^2}{4M_W^2} (N_e^0 - \bar{N}_e^0)(1 - c_A) + \frac{g^2 e B}{4M_W^4} (N_e - \bar{N}_e) - \frac{e B g^2}{2M_W^4} \int_0^{\infty} \frac{dp_3}{2\pi^2} \sum_{n=0}^{\infty} (2 - \delta_{n,0}) \left[E_{\nu_e} (E_{e,n} - \frac{m^2}{E_{e,n}}) \delta_{n,0} + \frac{k_3 p_3^2}{E_{e,n}} \right] (f_{e,n} + \bar{f}_{e,n}). \quad (2.5)$$

In the magnetic field, the electron energy is given by

$$E_{e,n}^2 = (p_3^2 + m^2 + 2neB). \quad (2.6)$$

For electrons in the background we have $c_V = -\frac{1}{2} + 2 \sin^2 \theta_W$, $c_A = \frac{1}{2}$, m is the electron mass and B is the constant background magnetic field. In Eq. (2.1), ϕ is the angle between the neutrino momentum and the direction of the magnetic field ($\mathbf{k} \cdot \mathbf{B}$). We will be considering the forward moving neutrinos (or moving along the magnetic field) and in rest of the paper consider $\phi \simeq 0$. Also for massless neutrino we assume $k_0 = k_3 = E_\nu$. For neutrinos propagating in the forward direction the last term in the Eq.(2.1) vanishes. Also for the strong magnetic field case, when only the lowest Landau level ($n = 0$) is populated the term $(a_{\parallel} - a_{\perp})$ vanishes. Thirdly even if the neutrinos are not propagating in the forward direction but the magnetic field is weak, then the term $(a_{\parallel} - a_{\perp})$ is very small. So we neglect its contribution in the rest of the paper and with this the effective potential can be given by

$$V_{\text{eff}} = b - c \cos \phi. \quad (2.7)$$

We shall assume that the magnetic field is weak ($B \ll m^2/e = B_c$) in the electron-positron plasma where the test neutrino is propagating. The electron density in a magnetized plasma is given by

$$\begin{aligned} N_e &= \frac{2eB}{4\pi^2} \sum_{n=0}^{\infty} (2 - \delta_{n,0}) \int_0^{\infty} dp_3 f_{e,n} \\ &= \frac{2eB}{4\pi^2} \left[2 \sum_{n=0}^{\infty} \int_0^{\infty} dp_3 f_{e,n} - \int_0^{\infty} dp_3 f_{e,0} \right], \end{aligned} \quad (2.8)$$

where we can further define

$$N_e^0 = \frac{2eB}{4\pi^2} \int_0^{\infty} dp_3 f_{e,0}. \quad (2.9)$$

We also assume that the chemical potential (μ) of the electrons and positrons are much smaller than their energy i.e. $\mu \ll E_e$. In this case the fermion distribution function can be written as a sum and is given by

$$f(E_e) = \frac{1}{e^{\beta(E_e - \mu)} + 1} \simeq \sum_{l=0}^{\infty} (-1)^l e^{-\beta(E_e - \mu)(l+1)}. \quad (2.10)$$

Using the above distribution function, the electron number density in the weak field limit is

$$N_e = \frac{m^3}{2\pi^2} \sum_{l=0}^{\infty} (-1)^l e^{\alpha} \left[\frac{2}{\sigma} K_2(\sigma) - \frac{B}{B_c} K_1(\sigma) \right], \quad (2.11)$$

and

$$N_e^0 = \frac{1}{2\pi^2} \frac{B}{B_c} m^3 \sum_{l=0}^{\infty} (-1)^l e^{\alpha} K_1(\sigma). \quad (2.12)$$

where we have defined

$$\begin{aligned} \alpha &= \beta\mu(l+1), \\ \sigma &= \beta m(l+1), \end{aligned} \quad (2.13)$$

and K_i is the modified Bessel function of integral order i . With the help of above, for an electron neutrino propagating in the medium, the Lorentz scalars b and c are expressed as

$$\begin{aligned} b &= b_0 - \frac{4\sqrt{2}}{\pi^2} G_F \left(\frac{m}{M_W} \right)^2 m^2 E_{\nu_e} \sum_{l=0}^{\infty} (-1)^l \cosh \alpha \left[\left(\frac{3}{\sigma^2} - \frac{1}{4} \frac{B}{B_c} \right) K_0(\sigma) + \left(1 + \frac{6}{\sigma^2} \right) \frac{K_1(\sigma)}{\sigma} \right], \\ c &= c_0 - \frac{4\sqrt{2}}{\pi^2} G_F \left(\frac{m}{M_W} \right)^2 m^2 E_{\nu_e} \sum_{l=0}^{\infty} (-1)^l \cosh \alpha \frac{1}{\sigma^2} \left(K_0(\sigma) + \frac{2}{\sigma} K_1(\sigma) \right), \end{aligned} \quad (2.14)$$

where

$$\begin{aligned} b_0 &= \sqrt{2} G_F \left[(N_e - \bar{N}_e)(1 + c_V) + \frac{B}{B_c} \left(\frac{m}{M_W} \right)^2 (N_e^0 - \bar{N}_e^0) \right], \\ c_0 &= \sqrt{2} G_F \left[(N_e^0 - \bar{N}_e^0)(1 - c_A) + \frac{B}{B_c} \left(\frac{m}{M_W} \right)^2 (N_e - \bar{N}_e) \right]. \end{aligned} \quad (2.15)$$

For muon and tau neutrinos, only the neutral current interaction will contribute. So for $\nu_{\mu,\tau}$ only c_V and c_A terms will contribute. For anti-neutrino, $(N_e^0 - \bar{N}_e^0)$ will be replaced by $-(N_e^0 - \bar{N}_e^0)$ and similarly $(N_e - \bar{N}_e)$ by $-(N_e - \bar{N}_e)$. For our convenience we can also define

$$N_e^0 - \bar{N}_e^0 = \frac{m^3}{\pi^2} \frac{B}{B_c} \sum_{l=0}^{\infty} (-1)^l \sinh \alpha K_1(\sigma) = \frac{m^3}{\pi^2} \Phi_1, \quad (2.16)$$

and

$$N_e - \bar{N}_e = \frac{m^3}{\pi^2} \sum_{l=0}^{\infty} (-1)^l \sinh \alpha \left[\frac{2}{\sigma} K_2(\sigma) - \frac{B}{B_c} K_1(\sigma) \right] = \frac{m^3}{\pi^2} \Phi_2. \quad (2.17)$$

In the weak field limit, the effect of magnetic field is very small in $N_e - \bar{N}_e$ and it is important when $B \gg B_c$. Due to the weak field limit, the magnetic field contribution is very much suppressed which is shown in Eq. (2.17). But in strong field limit, which is described in the next section, the number density is proportional to the magnetic field Eq. (2.16).

III. VERY STRONG FIELD LIMIT

For very strong magnetic field, only the lowest Landau Level (LL) $n = 0$ will contribute and in this case the energy of the particle is independent of the magnetic field and can be given by

$$E^2 = (p_3^2 + m^2), \quad (3.1)$$

and the number density of electrons is given by Eq. (2.12). Defining the particle asymmetry in the background as

$$L_i = \frac{(N_i - \bar{N}_i)}{N_\gamma}, \quad (3.2)$$

and also we have define L_i^0 when the particles are in LL. where $N_\gamma = 2/\pi^2 \xi(3) T^3$ is the photon number density, we can express

$$\begin{aligned} b_0 &= \sqrt{2} G_F N_\gamma \left[L_e (1 + c_V) + \frac{B}{B_c} \left(\frac{m}{M_W} \right)^2 L_e^0 \right], \\ c_0 &= \sqrt{2} G_F N_\gamma \left[L_e^0 (1 - c_A) + \frac{B}{B_c} \left(\frac{m}{M_W} \right)^2 L_e \right], \end{aligned} \quad (3.3)$$

and the potential can be written as

$$\begin{aligned} V &= \sqrt{2} G_F N_\gamma L_e^0 \left[1 + c_V + \frac{B}{B_c} \left(\frac{m}{M_W} \right)^2 - \left(1 - c_A + \frac{B}{B_c} \left(\frac{m}{M_W} \right)^2 \right) \cos \phi \right] \\ &\quad - \frac{2\sqrt{2}}{\pi^2} G_F \frac{B}{B_c} \left(\frac{m}{M_W} \right)^2 m^2 E_\nu \sum_{l=0}^{\infty} (-1)^l \cosh \alpha \left[\left(\frac{3}{2} K_0(\sigma) + \frac{2}{\sigma} K_1(\sigma) \right) - \frac{K_1(\sigma)}{\sigma} \cos \phi \right]. \end{aligned} \quad (3.4)$$

For forward moving neutrinos, the potential is simplified to

$$\begin{aligned} V &= \sqrt{2} G_F N_\gamma L_e^0 (c_V + c_A) \\ &\quad - \frac{2\sqrt{2}}{\pi^2} G_F \frac{B}{B_c} \left(\frac{m}{M_W} \right)^2 m^2 E_\nu \sum_{l=0}^{\infty} (-1)^l \cosh \alpha \left(\frac{3}{2} K_0(\sigma) + \frac{K_1(\sigma)}{\sigma} \right). \end{aligned} \quad (3.5)$$

This is the potential for ν_e propagating in the strongly magnetized e^-e^+ plasma (c_V and c_A are already defined for electron background), whereas for ν_μ and ν_τ the last term is absent which is order of magnitude suppressed. So for a system where lepton asymmetry is non-zero one can neglect the second term. In this situation the active-active neutrino oscillation is very much suppressed due to the cancellation of the leading order term. The magnetars or anomalous X-ray pulsars (AXPs) are believed to have magnetic field much above the critical field $B \gg m^2/e$ and probably one can use the above potential to study the neutrino propagation in their magnetized environment.

IV. GRB PHYSICS

A fireball is formed due to the sudden release of copious amount of γ -rays into a compact region with a size $c\delta t \sim 100 - 1000$ km by creating an opaque $\gamma - e^-e^+$ plasma. In the fireball the γ s and pair plasma will thermalize with a temperature of about 3-10 MeV. Afterward the fireball will expand relativistically under its own pressure and cools adiabatically[1, 3, 5]. When the optical depth of photon is of order unity, the radiation emerges freely to the intergalactic medium. As stated above, we shall consider the fireball temperature in the range 3-10 MeV for our analysis.

Baryon load in the fireball is an outstanding issue. The fireball contains baryons both from the progenitor and the surrounding medium. The electrons associated with the matter (baryons) can increase the opacity, hence delaying the process of radiation emission. The baryons can be accelerated along with the fireball and convert part of the radiation energy into bulk kinetic energy. So the dynamics of the fireball crucially depends on the baryon content of it. But the baryon load of the fireball has to be low ($10^{-8}M_\odot - 10^{-5}M_\odot$) otherwise it will be Newtonian and there will be no GRB[1, 13].

Here we consider a CP-asymmetric γ and e^-e^+ fireball, where the excess of electrons come from the electrons associated with the baryons within the fireball. We have shown earlier for $B = 0$ case that for the active-active neutrino oscillation, the potential is independent of the baryonic contribution. However for active-sterile neutrino oscillation the potential does depend on the baryonic contribution[19].

The problem of magnetic field in the GRBs is outstanding[3]. There is no way to get the magnetic field information directly from the fireball. It is strongly believed in the GRB community that the γ -rays which we detect are mostly due to the synchrotron radiation of charged particles in the magnetic field although the strength of it is still unknown. But the field strength will be smaller than B_c , because even if the central engine is having very strong magnetic field, the magnetic field will decay as $\sim r^{-2}$ when the jet moves away from the central engine making it weak. Here we shall take the weak field approximation $B \ll B_c$ and study the oscillation of neutrinos in the fireball environment.

In a stellar collapse or merger of compact binaries 5-20 MeV neutrinos are produced that trigger the burst. Due to nucleonic bremsstrahlung and annihilation of e^-e^+ , neutrinos of all kinds are produced which has a low flux compared to the previous process. Also due to inverse beta decay process MeV neutrinos can be produced. Normally the 5-20 MeV neutrinos produced due to collapse or merger of compact binaries will go away before the fireball is formed. If the fireball is fed continuously with the late time ejecta powered by neutrinos from the accretion torus then some of these MeV neutrinos will propagate through the fireball which we have discussed in the introduction. So due to above neutrino production mechanisms whether external or internal to the fireball some of these neutrinos will propagate through the fireball and the fireball plasma being in an extreme condition may affect the propagation of these neutrinos through it.

The GRBs are also sources of very high energy neutrinos and gammas which are produced during different stages of its dynamical evolution. Bahcall and Meszaros[22] have shown that due to dynamical decoupling of neutron from the rest of the fireball plasma, inelastic collision of protons and neutrons will produce 5-10 GeV neutrinos and they estimate about 7 events per year in a km^3 detector (for redshift $z \simeq 1$). But production of these neutrinos crucially depends on the neutron content of the fireball.

Also two different mechanisms are discussed by Meszaros and Rees[23] for the production of 2-25 GeV neutrinos. In the first mechanism they show that if internal shocks occur below the radiation photosphere, rapid diffusion of neutrons in both parallel and transverse to the radial direction occurs and inelastic collision with the protons can give rise to pions and subsequently neutrinos of energy about 2 GeV. In the second mechanism, neutrons diffuse transversely from a slower outflow into a fast jet, at a height where the transverse inelastic optical depth of the jet is close to unity. This mechanism can produce neutrino energy of order 25 GeV. The km^3 detectors with sufficiently dense phototubes can be able to detect about 3-15 events per year for $z \geq 1$.

The high energy gamma radiation can also be observed from GRB by acceleration of high energy protons in the magnetic field and at the same time accelerated high energy protons can also produce very high energy neutrinos[24, 25] and gamma rays[26, 27, 28, 29] due to photo pion production as well as proton-proton collisions. All these photons and neutrinos are in principle observables with the present day detectors.

Here for simplicity we assume that the fireball is charge neutral $L_e = L_p$ and spherical with an initial radius $R \simeq (100 - 1000)$ km and it has equal number of protons and neutrons. Then the baryon load in the fireball can be given by

$$\begin{aligned} M_b &\simeq \frac{16}{3\pi}\xi(3)L_e T^3 R^3 m_p \\ &\simeq 2.23 \times 10^{-4} L_e T_{MeV}^3 R_7^3 M_\odot. \end{aligned} \quad (4.1)$$

where T_{MeV} is the fireball temperature expressed in MeV and R_7 is in units of 10^7 cm and m_p is the proton mass.

For ultra relativistic expansion of the fireball, we assume the baryon load in it to be in the range $10^{-8}M_{\odot} - 10^{-5}M_{\odot}$ which corresponds to lepton asymmetry in the range $8.1 \times 10^{-4}R_7^{-3} \leq L_e \leq 8.1 \times 10^{-1}R_7^{-3}$.

V. NEUTRINO OSCILLATION

Here we consider the neutrino oscillation process $\nu_e \leftrightarrow \nu_{\mu,\tau}$. The evolution equation for the propagation of neutrinos in the above medium is given by

$$i \begin{pmatrix} \dot{\nu}_e \\ \dot{\nu}_{\mu} \end{pmatrix} = \begin{pmatrix} V - \Delta \cos 2\theta & \frac{\Delta}{2} \sin 2\theta \\ \frac{\Delta}{2} \sin 2\theta & 0 \end{pmatrix} \begin{pmatrix} \nu_e \\ \nu_{\mu} \end{pmatrix}, \quad (5.1)$$

where $\Delta = \delta m^2/2E_{\nu}$, V is the potential difference between V_{ν_e} and $V_{\nu_{\mu}}$, (i. e. $V = V_{\nu_e} - V_{\nu_{\mu}}$), E_{ν} is the neutrino energy and θ is the neutrino mixing angle. The conversion probability for the above process at a given time t is given by

$$P_{\nu_e \rightarrow \nu_{\mu}(\nu_{\tau})}(t) = \frac{\Delta^2 \sin^2 2\theta}{\omega^2} \sin^2 \left(\frac{\omega t}{2} \right), \quad (5.2)$$

with

$$\omega = \sqrt{(V - \Delta \cos 2\theta)^2 + \Delta^2 \sin^2 2\theta}. \quad (5.3)$$

The potential for the above oscillation process is

$$V = \sqrt{2}G_F \frac{m^3}{\pi^2} \left[\Phi_1 - \Phi_2 \cos \phi + \frac{B}{B_c} \left(\frac{m}{M_W} \right)^2 (\Phi_2 - \Phi_1 \cos \phi) - \frac{4}{\pi^2} \left(\frac{m}{M_W} \right)^2 \frac{E_{\nu_e}}{m} (\Phi_3 - \Phi_4 \cos \phi) \right], \quad (5.4)$$

where we have defined

$$\begin{aligned} \Phi_3 &= \sum_{l=0}^{\infty} (-1)^l \cosh \alpha \left[\left(\frac{3}{\sigma^2} - \frac{1}{4} \frac{B}{B_c} \right) K_0(\sigma) + \left(1 + \frac{6}{\sigma^2} \right) \frac{K_1(\sigma)}{\sigma} \right], \\ \Phi_4 &= \sum_{l=0}^{\infty} (-1)^l \cosh \alpha \frac{1}{\sigma^2} \left[K_0(\sigma) + \frac{2}{\sigma} K_1(\sigma) \right], \end{aligned} \quad (5.5)$$

and Φ_1 and Φ_2 are defined in Eqs. (2.16) and (2.17). For $\phi \simeq 0$ and weak field limit the potential can be written as

$$V \simeq \sqrt{2}G_F \frac{m^3}{\pi^2} \left[\Phi_1 - \Phi_2 - \frac{4}{\pi^2} \left(\frac{m}{M_W} \right)^2 \frac{E_{\nu_e}}{m} (\Phi_3 - \Phi_4) \right]. \quad (5.6)$$

For anti-neutrinos the functions Φ_1 and Φ_2 will change signs. The oscillation length for the neutrino is given by

$$L_{osc} = \frac{L_v}{\sqrt{\cos^2 2\theta \left(1 - \frac{V}{\Delta \cos 2\theta} \right)^2 + \sin^2 2\theta}}, \quad (5.7)$$

where $L_v = 2\pi/\Delta$ is the vacuum oscillation length. For resonance to occur, we should have $V > 0$ and

$$V = \Delta \cos 2\theta. \quad (5.8)$$

The resonance length can be given by

$$L_{res} = \frac{L_v}{\sin 2\theta}. \quad (5.9)$$

The positivity of the potential implies that the chemical potential μ of the background electrons and positrons should not be zero, so that the difference of the number densities of the particles and anti-particles as shown in Eqs. (2.16)

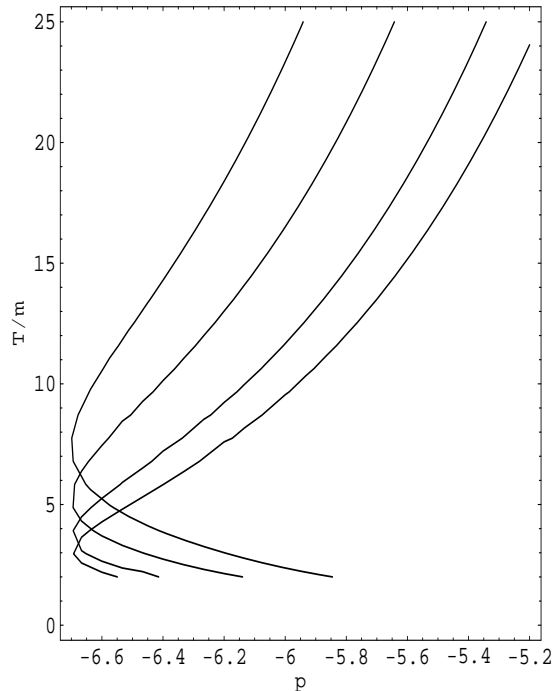


FIG. 1: For the best fit value of the SNO data $\delta m^2 \sim 7.1 \times 10^{-5} eV^2$ and $\sin^2 2\theta \sim 0.69$ we have the contour plot for p and T/m (where $\mu = 10^p m$) satisfying the resonance condition for four different neutrino energies 5, 10, 20 and 30 MeV from left to right respectively. Here we have taken $B/B_c = 0.1$.

and (2.17) will be non vanishing. Also μ should not be very small, otherwise the potential will be negative. The resonance condition is

$$\Phi_1 - \Phi_2 - 3.196 \times 10^{-11} E_{MeV} (\Phi_3 - \Phi_4) = 2.26 \frac{\delta \tilde{m}^2}{E_{MeV}} \cos 2\theta, \quad (5.10)$$

where $\delta \tilde{m}^2$ is expressed in units of eV^2 and the neutrino energy E_ν in units of MeV as E_{MeV} . The left hand side depends on μ , temperature T of the plasma and the neutrino energy. On the other hand the right hand side depends only on the neutrino energy (for a given set of neutrino mass square difference and the mixing angle). Let us emphasize that the resonance condition for $B = 0$ and $B \neq 0$ are different. In the $B = 0$ case for resonance condition to satisfy, first the lepton asymmetry has to satisfy the necessary condition $L_e > 6.14 \times 10^{-9} T_{MeV}^2$ [19], whereas the presence of magnetic field modifies this condition as shown in Eq. (5.10). In the magnetic field case, there is no explicit temperature dependence. Because of these modifications the magnetized plasma result is different from the $B = 0$ case. But the resonance length for both the situations are the same as the resonance length does not depend on the magnetic field.

We have found that at resonance the function Φ_2 is order of magnitude smaller than Φ_1 and $3.196 \times 10^{-11} E_{MeV} (\Phi_3 - \Phi_4)$ is of same order as Φ_1 . At the resonance for a given set of neutrino oscillation parameters δm^2 and $\sin^2 2\theta$, the resonance length only depends linearly on the neutrino energy. So the change in background temperature or number density in the fireball will not affect L_{res} . For our analysis we have taken three different neutrino energies $E_\nu = 5, 10$ and 20 MeV and for each neutrino energy three different fireball temperatures $T = 3, 5$ and 10 MeV are taken. We take into account the neutrino oscillation parameters from solar, atmospheric (SNO and SuperKamiokande), and the Liquid Scintillator Neutrino Detector (LSND) reactor neutrinos to study the resonance conditions in the fireball. The resonance oscillation of neutrinos can constrain the fireball parameters. For the best fit neutrino oscillation parameter sets δm^2 and $\sin^2 2\theta$ of the above three different state of the art experiments (SNO, Super Kamiokande and LSND), we have shown what should be the values of μ and T to satisfy the resonance condition for different neutrino energies in the fireball plasma. Afterward these values of μ and T are used to calculate the lepton asymmetry L_e , baryon load M_b and the resonance length L_{res} of the propagating neutrinos.

In Fig.1 we have shown the values of μ and T which satisfy the resonance condition for four different neutrino energies 5, 10, 20 and 30 MeV respectively by taking into account the best fit values of δm^2 and $\sin^2 2\theta$ from SNO for

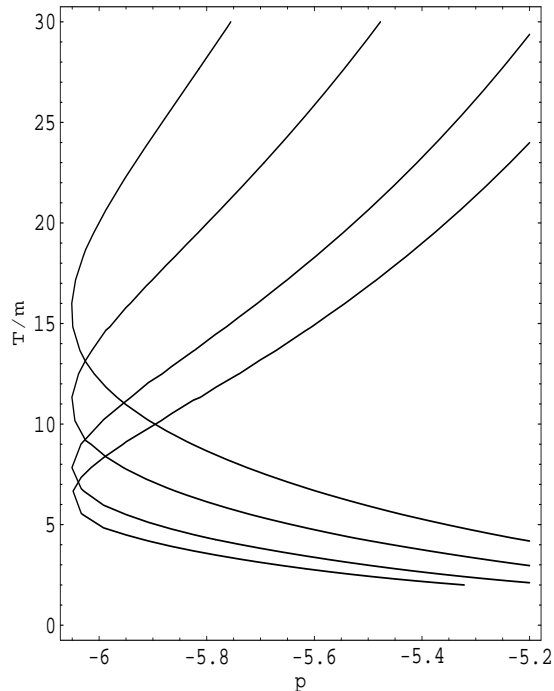


FIG. 2: The contour plot satisfying the resonance condition for the Super-Kamiokande neutrino oscillation parameters $\delta m^2 \sim 2.5 \times 10^{-3} eV^2$ and $\sin^2 2\theta \sim 0.9$, for different p and T/m are shown. The definitions of p is same as in Fig. 1 and also the same magnetic field is used. The four different curves from left to right are for 5, 10, 20 and 30 MeV neutrino energy respectively.

TABLE I: SNO: The best fit values of the neutrino oscillation parameters $\delta m^2 \sim 7.1 \times 10^{-5} eV^2$ and $\sin^2 2\theta \sim 0.69$ from the combined analysis of the salt phase data of SNO[30] and KamLAND[31] are used in the resonance condition for different neutrino energies in this table. The magnetic field used here is $B/B_c = 0.1$.

E_{MeV}	T(MeV)	L_e	$L_{res}(\text{cm})$	$M_b(R_7^3 M_\odot)$
5	3	3.28×10^{-8}	2.10×10^7	2.97×10^{-10}
	5	4.93×10^{-8}		9.14×10^{-10}
	10	5.07×10^{-8}		1.13×10^{-8}
10	3	4.71×10^{-8}	4.21×10^7	2.83×10^{-10}
	5	5.34×10^{-8}		1.49×10^{-9}
	10	9.99×10^{-8}		2.23×10^{-8}
20	3	6.83×10^{-8}	8.42×10^7	4.11×10^{-10}
	5	1.02×10^{-7}		2.85×10^{-9}
	10	1.99×10^{-7}		4.44×10^{-8}

fireball temperature in the range 3 to 10 MeV. In this range of temperatures it is shown that each value of chemical potential corresponds to two different temperatures, so we can tell that the temperature is degenerate. The increase in neutrino energy decreases the lower temperature for a particular μ and finally the temperature degeneracy goes away for high energy neutrinos. The same behavior is observed in the temperature and the chemical potential for the best fit Super Kamiokande result (δm^2 and $\sin^2 2\theta$) which is plotted in Fig.2. But for the combined LSND and KARMEN data Fig. 3 we have shown that there is no temperature degeneracy observed in the range of temperature (3-10 MeV) we consider. The degeneracy appears when the temperature goes above about 17 MeV, which is clearly seen in Fig. 3. Below we analyze our result for the above three experiments separately.

SNO: The salt phase data of SNO from solar neutrino[30], combined with the KamLAND[31] reactor anti-neutrino results constraint the neutrino oscillation parameters and are given by $6 \times 10^{-5} eV^2 < \delta m^2 < 10^{-4} eV^2$ and $0.64 < \sin^2 2\theta < 0.96$. The best fit point for the above data is obtained for $\delta m^2 \sim 7.1 \times 10^{-5} eV^2$ and $\sin^2 2\theta \sim 0.69$ with 99% confidence level . We have used this best fit point for the resonance condition for different neutrino energies and

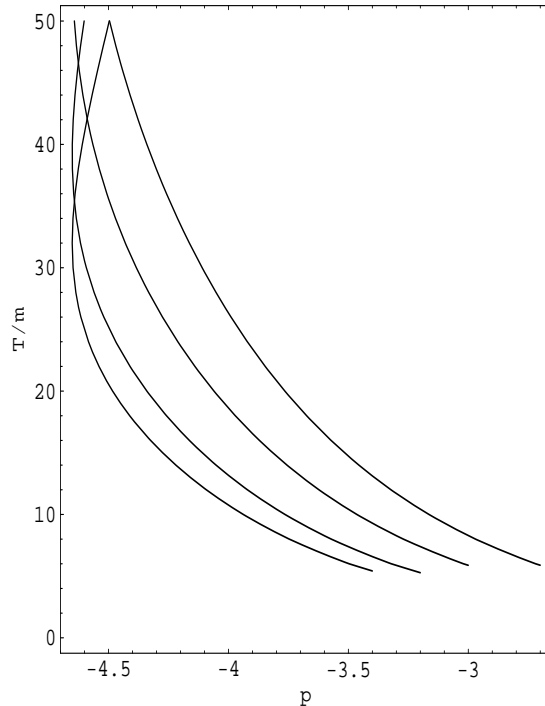


FIG. 3: This is for the LSND oscillation parameters $\delta m^2 \sim 0.5 eV^2$ and $\sin^2 2\theta \sim 0.0049$ and all other parameters are the same as in Fig. 1 but the 5, 10, 20, 30 MeV curves are from right to left.

TABLE II: SK: The best fit values of the atmospheric neutrino oscillation parameters $\delta m^2 \sim 2.5 \times 10^{-3} eV^2$ and $\sin^2 2\theta \sim 0.9$ from Super-Kaminkande Collaboration[32] are used in the resonance condition for different neutrino energies in this table. The magnetic field we have taken here is $B/B_c = 0.1$.

E_{MeV}	T(MeV)	L_e	$L_{res}(cm)$	$M_b(R_7^3 M_\odot)$
5	3	7.04×10^{-7}	522763	4.24×10^{-9}
	5	1.73×10^{-7}		4.83×10^{-9}
	10	6.92×10^{-8}		1.54×10^{-8}
10	3	3.81×10^{-7}	1.05×10^6	2.30×10^{-9}
	5	1.30×10^{-7}		3.62×10^{-9}
	10	1.09×10^{-7}		2.44×10^{-8}
20	3	2.38×10^{-7}	2.09×10^6	1.44×10^{-9}
	5	1.37×10^{-7}		3.81×10^{-9}
	10	2.04×10^{-7}		4.54×10^{-8}

the observables are given in TABLE I. For neutrino energy 5 MeV and the fireball temperature 3 MeV, the lepton asymmetry is $L_e \sim 3.28 \times 10^{-8}$, $L_{res} \sim 210$ km and $M_b \sim 2.97 \times 10^{-10} R_7^3 M_\odot$. If the fireball radius is 100 Km, then the resonance length is longer than the size of the fireball and also the baryon load is too low. The baryon load problem can be resolved by increasing the fireball radius, but neutrino can just oscillate because still the resonance length is quite large.

Going from 5 MeV neutrinos to 20 MeV neutrinos and background temperature from 3 MeV to 10 MeV, we have $L_e \sim 2 \times 10^{-7}$, $M_b \sim 4.44 \times 10^{-8} R_7^3 M_\odot$ and $L_{res} \sim 842$ km. For higher energy neutrinos the resonance length is so large that even if we increase the radius to 1000 km, there is hardly any resonant oscillation of neutrino within the fireball. So for neutrino oscillation parameters in the solar neutrino range (SNO) there is hardly any resonant oscillation.

SuperKaminkande: The atmospheric neutrino oscillation parameters reported by the Super-Kamiokande (SK) Collaboration[32] are in the range $1.9 \times 10^{-3} eV^2 < \delta m^2 < 3.0 \times 10^{-3} eV^2$ and $0.9 \leq \sin^2 2\theta \leq 1.0$ with a 90% confidence level. In this parameter space we consider the good fit point $\delta m^2 \sim 2.5 \times 10^{-3} eV^2$ and $\sin^2 2\theta \sim 0.9$ to

TABLE III: LSND: The best fit values of the neutrino oscillation parameters $\delta m^2 \sim 0.5 eV^2$ and $\sin^2 2\theta \sim 0.0049$ from LSND and KARMEN[33] are used in the resonance condition for different neutrino energies. The magnetic field we have taken is $B/B_c = 0.1$.

E_{MeV}	T(MeV)	L_e	L_{res} (cm)	$M_b(R_7^3 M_\odot)$
5	3	4.77×10^{-4}	35424.1	2.87×10^{-6}
	5	9.38×10^{-5}		2.62×10^{-6}
	10	1.23×10^{-5}		2.74×10^{-6}
10	3	2.27×10^{-4}	70848.1	1.37×10^{-6}
	5	4.77×10^{-5}		1.33×10^{-6}
	10	6.36×10^{-6}		1.42×10^{-6}
20	3	1.18×10^{-4}	141696	7.11×10^{-7}
	5	2.46×10^{-5}		6.85×10^{-7}
	10	3.28×10^{-6}		7.32×10^{-7}

study the resonance condition in the GRB fireball . The result of our analysis is given in TABLE II.

For neutrino energy in the range 5 to 20 MeV and background temperature in the range 3 to 10 MeV, there is not much variation in L_e but some variation in L_{res} and in M_b is observed. For neutrino energy 5 MeV and fireball temperature 5 MeV we have $L_e \sim 1.73 \times 10^{-7}$ and $L_{res} \sim 5.2$ km . Similarly for neutrino energy 10 MeV and fireball temperature 10 MeV, the $L_{res} \sim 10.5$ km, which is twice the one for neutrino energy 5 MeV. For 20 MeV neutrinos we obtain $L_{res} \sim 21$ km. This is because for a given set of neutrino oscillation parameters the resonance length is proportional to neutrino energy and does not depends on other factors. Also the baryon content in the fireball is proportional to T^3 . So for a given neutrino energy, background with high temperature has more baryon content than the low temperature one. The low value of M_b can be adjusted within $10^{-8} M_\odot$ to $10^{-5} M_\odot$ by adjusting the R_7 . Both the L_{res} and L_e are within the range of value we would expect and with this L_{res} , before coming out of the fireball, the neutrino can oscillate many times resonantly from one species to another.

LSND: Finally we consider the reactor neutrino data from LSND and KARMEN[33] to study the resonant oscillation of neutrino in the fireball medium. The combined analysis of both LSND and KARMEN 2 give the oscillation parameters in the range $0.45 eV^2 < \delta m^2 < 1 eV^2$ and $2 \times 10^{-3} < \sin^2 2\theta < 7 \times 10^{-3}$ with a 90% confidence level. For our analysis we consider $\delta m^2 \sim 0.5 eV^2$ and $\sin^2 2\theta \sim 0.0049$ given in TABLE III. In this case the L_e and M_b are much higher compared to the one in SNO and SK. But the resonance length is much smaller than both SNO and SK. For a 10 MeV neutrino propagating in 5 MeV background temperature fireball plasma, we have $L_e \sim 4.77 \times 10^{-5}$, $L_{res} \sim 0.7$ km and $M_b \sim 1.33 \times 10^{-6} R_7^3 M_\odot$ and for neutrino energy 20 MeV and background temperature 10 MeV, we obtain $L_e \sim 3.28 \times 10^{-6}$, $L_{res} \sim 1.4$ km and $M_b \sim 7.32 \times 10^{-7} R_7^3 M_\odot$. As the L_{res} is much smaller compared to the size of the fireball, the propagating neutrinos will resonantly oscillate before coming out of the fireball medium.

VI. CONCLUSIONS

We have studied the active-active neutrino oscillation process $\nu_e \leftrightarrow \nu_{\mu,\tau}$ in the weakly magnetized e^-e^+ plasma of the GRB fireball assuming it to be spherical with a radius of 100 to 1000 km and temperature in the range 3-10 MeV. We further assume that the fireball is charge neutral due to the presence of protons and their accompanying electrons. The baryon load of the fireball is solely due to the presence of almost equal number of protons and neutrons in it. The effective potential for $\nu_e \leftrightarrow \nu_{\mu,\tau}$ oscillation does not depend on the baryon content of the fireball, simply because the neutral current contribution to the neutrino potential is same for ν_e and $\nu_{\mu,\tau}$. By assuming charge neutral fireball we have $L_e = L_p$, which we have used to calculate the baryon content of the fireball.

We have used the best fit values of the neutrino oscillation parameters from solar, atmospheric and reactor neutrinos and studied the resonance condition for the above oscillation process and calculated the lepton asymmetry, resonance length and the baryon content of the fireball for neutrinos of energy 5, 10 and 20 MeV and fireball temperature of 3, 5 and 10 MeV. We have shown that for δm^2 and $\sin^2 2\theta$ in the solar neutrino (from SNO) range, the resonance length is large compared to the size of the fireball which increases with the increase of the neutrino energy and also the baryon load is low. In this case, probably a few or no resonant oscillation will take place. But if the δm^2 and $\sin^2 2\theta$ are in the atmospheric (SK) or in the reactor neutrino range, there can be many oscillation before the neutrinos come out of the fireball, so that the average conversion probability of neutrinos will be ~ 0.5 . We have also shown that in these two cases (SK and LSND), the baryon load of the fireball is neither very low nor very high. A detail study of the neutrino propagation in the GRB fireball is necessary to understand the finer detail of the fireball dynamics. Also

this depends on the content of the fireball i.e. how much baryon it contains and may affect the dynamics of the jet.

The GRBs can be detected through GeV or higher energy neutrinos as well as high energy gamma rays with the present day neutrino and gamma-ray detectors. All these neutrinos and gammas are produced after the prompt emission of MeV photons. But these MeV neutrinos due to the collapse of a type I b,c supernova is similar to the one produced by type II supernova (for example SN1987A) and are of cosmological distance. These cosmological events make the MeV neutrino flux very low on earth compared to the one which we had seen from the supernova SN1987A. Also low energy neutrinos have very low cross section and combine with the cosmological distance (low flux) makes the required detector volume extremely large. So with the present generation neutrino telescopes it is very difficult to detect these low energy neutrinos.

ACKNOWLEDGMENTS

We are thankful to B. Zhang for many useful discussions. Y.Y. K and S. S. thank S. P. Kim and APCTP for a kind hospitality where this work has been initiated. The Work of S. S. is partially supported by DGAPA-UNAM (Mexico) project IN101409. Y.Y.K's work is partially supported by KIAS and APCTP in Korea.

-
- [1] T. Piran, Phys. Rept. **314** (1999) 575 [arXiv:astro-ph/9810256].
 - [2] B. Zhang, Chin. J. Astron. Astrophys. **7**, 1 (2007) [arXiv:astro-ph/0701520].
 - [3] B. Zhang and P. Meszaros, Int. J. Mod. Phys. A **19**, 2385 (2004) [arXiv:astro-ph/0311321].
 - [4] T. Piran, Phys. Rept. **333**, 529 (2000) [arXiv:astro-ph/9907392].
 - [5] P. Meszaros, Nucl. Phys. Proc. Suppl. **80**, 63 (2000) [arXiv:astro-ph/9904038].
 - [6] M. Ruffert and H. T. Janka, Astron. Astrophys. **344**, 573 (1999) [arXiv:astro-ph/9809280].
 - [7] N. Gehrels *et al.*, Nature **437**, 851 (2005) [arXiv:astro-ph/0505630].
 - [8] S. D. Barthelmy *et al.*, Nature **438**, 994 (2005) [arXiv:astro-ph/0511579].
 - [9] J. S. Villaseñor *et al.*, Nature **437**, 855 (2005) [arXiv:astro-ph/0510190].
 - [10] V. V. Usov, Nature **357**, 472 (1992).
 - [11] D. A. Uzdensky and A. I. MacFadyen, Phys. Plasmas **14**, 056506 (2007) [arXiv:0707.0576 [astro-ph]].
 - [12] J. Goodman, Astrophys. J. **308** (1986) L47.
 - [13] E. Waxman, Lect. Notes Phys. **598** (2003) 393 [arXiv:astro-ph/0303517].
 - [14] B. Zhang *et al.*, Astrophys. J. **642**, 354 (2006) [arXiv:astro-ph/0508321].
 - [15] D. N. Burrows *et al.*, Science **309**, 1833 (2005) [arXiv:astro-ph/0506130].
 - [16] G. G. Raffelt, Astrophys. J. **561**, 890 (2001) [arXiv:astro-ph/0105250].
 - [17] K. Enqvist, K. Kainulainen and J. Maalampi, Nucl. Phys. B **349**, 754 (1991).
 - [18] S. Sahu and V. M. Bannur, Phys. Rev. D **61**, 023003 (2000) [arXiv:hep-ph/9806427].
 - [19] S. Sahu and J. C. D'Olivo, Phys. Rev. D **71**, 047303 (2005) [arXiv:hep-ph/0502043].
 - [20] A. Bravo Garcia and S. Sahu, Mod. Phys. Lett. A **22** (2007) 213.
 - [21] A. Bravo Garcia, K. Bhattacharya and S. Sahu, Mod. Phys. Lett. A **23**, 2771 (2008) [arXiv:0706.3921 [hep-ph]].
 - [22] J. N. Bahcall and P. Meszaros, Phys. Rev. Lett. **85** (2000) 1362 [arXiv:hep-ph/0004019].
 - [23] P. Meszaros and M. J. Rees, Astrophys. J. **541** (2000) L5 [arXiv:astro-ph/0007102].
 - [24] E. Waxman and J. N. Bahcall, Phys. Rev. Lett. **78** (1997) 2292 [arXiv:astro-ph/9701231].
 - [25] . R. Abbasi [IceCube Collaboration], arXiv:0902.0131 [astro-ph.HE].
 - [26] D. C. Morris *et al.*, Astrophys. J. **654**, 413 (2006) [arXiv:astro-ph/0602490].
 - [27] A. Galli and L. Piro, arXiv:0805.2884 [astro-ph].
 - [28] A. A. Abdo *et al.* [Fermi LAT and Fermi GBM Collaborations], Science **323** (2009) 1688.
 - [29] A. Corsi, D. Guetta and L. Piro, arXiv:0905.1513 [astro-ph.CO].
 - [30] S. N. Ahmed *et al.* [SNO Collaboration], Phys. Rev. Lett. **92**, 181301 (2004) [arXiv:nucl-ex/0309004].
 - [31] T. Araki *et al.* [KamLAND Collaboration], Phys. Rev. Lett. **94**, 081801 (2005) [arXiv:hep-ex/0406035].
 - [32] Y. Ashie *et al.* [Super-Kamiokande Collaboration], Phys. Rev. Lett. **93**, 101801 (2004) [arXiv:hep-ex/0404034].
 - [33] E. D. Church, K. Eitel, G. B. Mills and M. Steidl, Phys. Rev. D **66**, 013001 (2002) [arXiv:hep-ex/0203023].